




Ehrlichia Isolate from a Minnesota Tick: Characterization and Genetic Transformation

 Geoffrey E. Lynn,^{a*} Nicole Y. Burkhardt,^a Roderick F. Felsheim,^b Curtis M. Nelson,^a Jonathan D. Oliver,^{a*} Timothy J. Kurtti,^a Ingrid Cornax,^{c*} M. Gerard O'Sullivan,^c Ulrike G. Munderloh^a

^aDepartment of Entomology, University of Minnesota—Twin Cities, Minneapolis, Minnesota, USA

^bRoderick Felsheim LLC, St. Paul, Minnesota, USA

^cComparative Pathology Shared Resource, University of Minnesota—Twin Cities, Minneapolis, Minnesota, USA

ABSTRACT *Ehrlichia muris* subsp. *eaucloirensis* is recognized as the etiological agent of human ehrlichiosis in Minnesota and Wisconsin. We describe the culture isolation of this organism from a field-collected tick and detail its relationship to other species of *Ehrlichia*. The isolate could be grown in a variety of cultured cell lines and was effectively transmitted between *Ixodes scapularis* ticks and rodents, with PCR and microscopy demonstrating a broad pattern of dissemination in arthropod and mammalian tissues. Conversely, *Amblyomma americanum* ticks were not susceptible to infection by the *Ehrlichia*. Histologic sections further revealed that the wild-type isolate was highly virulent for mice and hamsters, causing severe systemic disease that was frequently lethal. A *Himar1* transposase system was used to create mCherry- and mKate-expressing EmCRT mutants, which retained the ability to infect rodents and ticks.

IMPORTANCE Ehrlichioses are zoonotic diseases caused by intracellular bacteria that are transmitted by ixodid ticks. Here we report the culture isolation of bacteria which are closely related to, or the same as the *Ehrlichia muris* subsp. *eaucloirensis*, a recently recognized human pathogen. EmCRT, obtained from a tick removed from deer at Camp Ripley, MN, is the second isolate of this subspecies described and is distinctive in that it was cultured directly from a field-collected tick. The isolate's cellular tropism, pathogenic changes caused in rodent tissues, and tick transmission to and from rodents are detailed in this study. We also describe the genetic mutants created from the EmCRT isolate, which are valuable tools for the further study of this intracellular pathogen.

KEYWORDS *Amblyomma americanum*, *Ehrlichia*, *Ehrlichia muris*, *Himar1*, *Ixodes scapularis*, cell culture

In recent decades, the North Central region of the United States has been identified as a focal area for emerging tick-borne diseases, most of which are caused by pathogens transmitted by the black-legged tick, *Ixodes scapularis* (1–3). Lyme disease, the most common vector-borne disease in the United States (4), and human anaplasmosis (HA), first described in patients from Minnesota and western Wisconsin in the early 1990s (5, 6), are the most frequently diagnosed tick-borne illnesses in the region (7, 8). Other human pathogens transmitted by black-legged ticks in these states include *Babesia microti*, *Borrelia miyamotoi*, Powassan virus, and most recently, *Borrelia mayonii* (2, 9).

In 2009, *Ehrlichia muris*, previously not considered to be a human pathogen in North America, was identified as the cause of illness in Minnesota and Wisconsin patients (10). As of 2018, more than 115 human cases of ehrlichiosis attributed to the recently named *Ehrlichia muris* subsp. *eaucloirensis* (formerly referred to as the *Ehrlichia muris*-like agent [EMLA]) (11) have been reported, though this figure likely underrepresents true inci-

Citation Lynn GE, Burkhardt NY, Felsheim RF, Nelson CM, Oliver JD, Kurtti TJ, Cornax I, O'Sullivan MG, Munderloh UG. 2019. *Ehrlichia* isolate from a Minnesota tick: characterization and genetic transformation. *Appl Environ Microbiol* 85:e00866-19. <https://doi.org/10.1128/AEM.00866-19>.

Editor Charles M. Dozois, INRS—Institut Armand-Frappier

Copyright © 2019 American Society for Microbiology. All Rights Reserved.

Address correspondence to Geoffrey E. Lynn, geoffrey.lynn@yale.edu.

* Present address: Geoffrey E. Lynn, Section of Infectious Diseases, Department of Internal Medicine, School of Medicine, Yale University, New Haven, Connecticut, USA; Jonathan D. Oliver, Division of Environmental Health Sciences, School of Public Health, University of Minnesota Twin Cities, Minneapolis, Minnesota, USA; Ingrid Cornax, Division of Host-Microbe Systems and Therapeutics, Department Pediatrics, Skaggs School of Pharmacy and Pharmaceutical Sciences, University of California, San Diego, California, USA.

Received 16 April 2019

Accepted 2 May 2019

Accepted manuscript posted online 10 May 2019

Published 1 July 2019

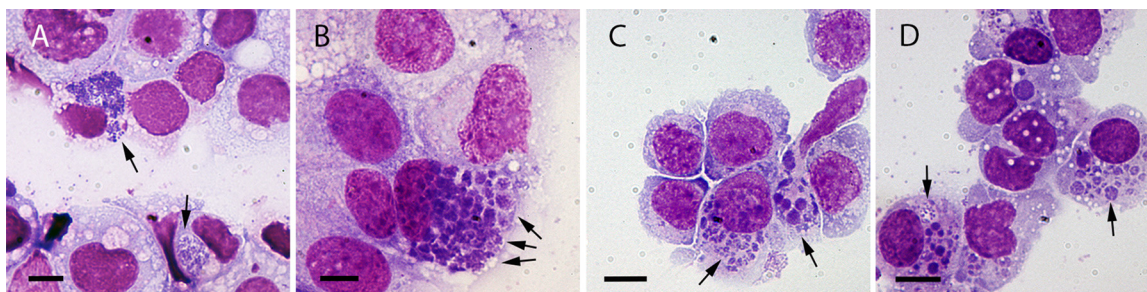


FIG 1 Cultured cells infected with EmCRT, fixed and stained with Giemsa solution. Arrows indicate ehrlichial morulae, which stain a darker shade of purple than host cells. (A) ISE6; (B) RF/6A; (C) HL-60; (D) THP1. Scale bars, 10 μ m.

dence given the nonspecific clinical features of disease and limited use of specific diagnostic testing for *E. muris* (12, 13). Interestingly, transmission to humans appears to be limited to Minnesota and Wisconsin, though a related subspecies of *E. muris* is found in the northeastern United States (14).

Given its recent discovery and relative scarcity, the natural ecology of *E. muris eaulairensis* is only partially understood at present. *Ixodes scapularis* collected in Minnesota and Wisconsin has tested positive for *E. muris eaulairensis*, while American dog tick (*Dermacentor variabilis*) specimens from the same locations were negative (10, 15, 16). Experimental transmission and acquisition of *E. muris eaulairensis* by *I. scapularis* to and from mice are efficient (17–19), which suggests that this tick species is an important vector in nature, whereas *D. variabilis* was shown to be an incompetent vector (19). *Ehrlichia* spp. are not known to be vertically transmitted, and though white-footed mice (*Peromyscus leucopus*) both acquire *E. muris eaulairensis* infections in nature (20) and have been shown experimentally to be reservoir-competent hosts (21), the full extent of vertebrate species contributing to enzootic transmission is currently unknown.

We report here the culture isolation of *Ehrlichia muris* from a field-collected *I. scapularis* tick (17), with genotypic and histologic characterization indicating that it is very closely related to or the same as the *E. muris eaulairensis* (*Ehrlichia* sp., Wisconsin) isolated from a human patient (10). Also described is the genetic transformation of this organism using a *Himar1* transposition system, which resulted in mutants that expressed fluorescent protein markers *in vitro* and *in vivo*, allowing visual identification of infection in live tick tissues using confocal microscopy.

RESULTS

Propagation of the *Ehrlichia* isolate in cell culture and genotyping. After isolation of EmCRT in ISE6 cells (Fig. 1A), ehrlichiae were extracted from host cells and successfully grown in the following cell lines selected for their ability to support various *Ehrlichia* spp. (10, 21–25): RF/6A (Fig. 1B), HL-60, (Fig. 1C), THP-1 (Fig. 1D), DH82, and HMEC-1. In ISE6 cultures, ehrlichial inclusions frequently expanded to encompass a large part of the cytoplasm, developing into morulae that can contain dozens or hundreds of bacteria. Similar to the *E. muris* type species isolate (*E. muris* AS145), one or two large morulae per ISE6 cell were typically observed for EmCRT infection, in contrast to the *Ixodes ovatus Ehrlichia* (IOE) isolate, which forms multiple smaller morulae in this cell line (26).

In early-stage infection (ca. 12 to 24 h) of HL-60 and THP-1 cells, individual cells contained one or two small morulae, while cells later stages of infection (24 to 48 h) harbored many equally small morulae. RF/6A and DH82 cells also maintained small morulae, which increased in quantity until the entire cell was packed with numerous small to mid-sized morulae. In several instances, a morula was observed within a tick cell nucleus by either Giemsa stain or live confocal microscopy, an observation that has also been reported for *E. chaffeensis* (27). Yet another distinctive characteristic of this isolate was that in adherent mammalian cell cultures, advanced ehrlichial infection

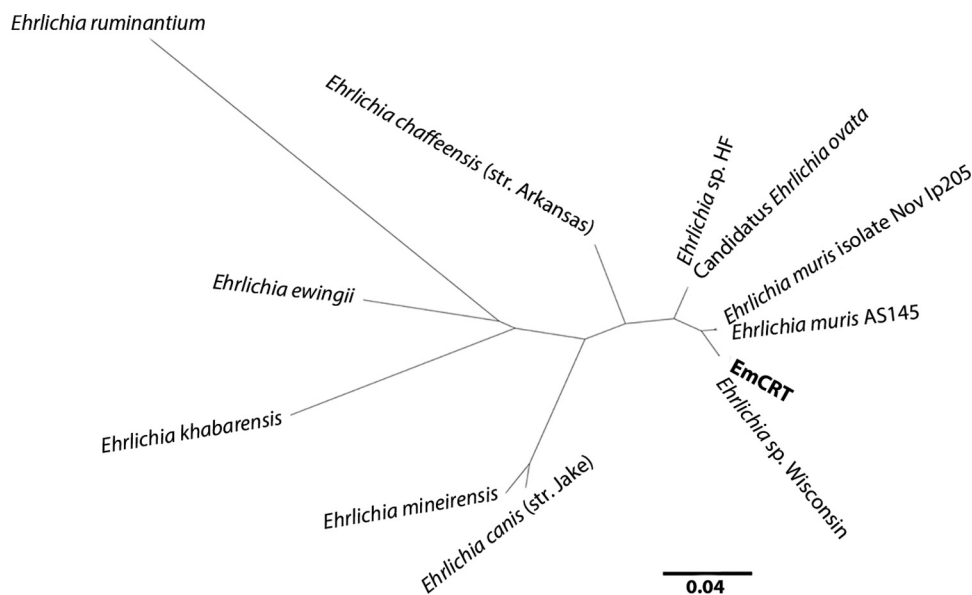


FIG 2 Phylogenetic tree showing the relationship between EmCRT and closely related *Ehrlichia* compared by *groESL* sequence. EmCRT is identical to the human *E. muris eaucloirensis* isolate (*Ehrlichia sp. Wisconsin*), as are each of two pairs of Asian isolates (*Ehrlichia muris* AS145/*Ehrlichia muris* isolate Nov Ip205 and “*Candidatus Ehrlichia ovata*”/*Ehrlichia sp. strain HF*). Node values indicating the probability that branches are correctly arranged were calculated and were all 96% or greater, with the exception of the *E. ruminantium*-*E. ewingii* node, which was 52%. The scale bar denotes the expected site changes per distance.

resulted in cell rounding and detachment from the flask. These were attributed to degeneration of the actin cytoskeleton and were readily observed in infected GFP-LifeAct-expressing RF/6A cells.

A phylogenetic tree (Fig. 2) showing the genetic relationship of selected *Ehrlichia* spp. closely related to EmCRT was constructed with *groESL* sequences. Probability values for each of the nodes were 96% or greater, with the exception of the *E. ruminantium*-*E. ewingii* node (52%). Our isolate matched the human-derived *E. muris eaucloirensis* isolate (*Ehrlichia sp. Wisconsin*) and was closely related to two *E. muris* isolates from Asia (*E. muris* AS145 and *E. muris* isolate Nov Ip205). The “*Candidatus Ehrlichia ovata*” and *Ehrlichia sp. HF* sequences were also indistinguishable from each other.

Rodent infection and histology. Infection of mice and hamsters with EmCRT produced severe and often fatal systemic disease, with disease outcome influenced by route of inoculation, quantity and *in vitro* passage number of inocula, and host animal attributes, such as age and species. Use of a larger inoculum, a low passage number of EmCRT culture, and younger animals were each more likely to result in lethal infections, as was the use of hamsters as opposed to C57BL/6 mice. Signs of illness included hunched posture, huddling, dyspnea, tachypnea, inactivity, ruffled fur, and ataxia, with rapid onset less than 24 h prior to fatal outcome. In fatal cases, animals typically expired between 9 and 13 days postinoculation (dpi) and necropsies of moribund animals revealed moderate splenomegaly and pleural effusions consisting of cloudy, pale yellow serous fluid. In contrast to healthy lung tissues, which typically float for several hours in buffered formalin solution, lung tissues from animals in late stages of disease sank immediately into the fixative, indicating pulmonary consolidation. Examination of histological sections of lung tissue revealed diffuse moderate to severe interstitial pneumonia (pneumonitis) with marked pulmonary edema consistent with diffuse alveolar damage (Fig. 3). The alveolar walls were diffusely thickened by increased numbers of predominantly mononuclear inflammatory cells and had multiple small foci of necrosis. There was also mild hemorrhage and increased numbers of alveolar macrophages. The spleen had disruption and focal necrosis of the white pulp which

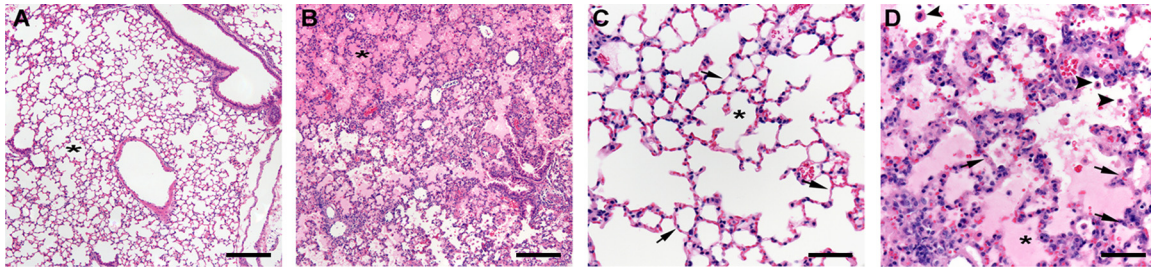


FIG 3 H&E-stained lung sections from C57BL/6 mice at 9 dpi. (A) Uninfected control displaying clear alveolar space (asterisk) and bronchioles. (B) Infected mouse. The lung has diffuse interstitial pneumonia and pulmonary edema (asterisk denotes alveolus filled with edema). (C) Higher magnification of the lung in an uninfected mouse. Note the thin alveolar walls (arrows) and the clear alveolar space (asterisk). (D) Higher magnification of the lung in an infected mouse. The alveolar septa (arrows) are diffusely thickened and hypercellular. The alveoli are edematous (asterisk) and contain increased numbers of alveolar macrophages (arrowheads). Scale bars: 200 μm (A and B) and 50 μm (C and D).

was infiltrated by plasma cells and other large lymphoid cells; similar cellular infiltrates were present throughout the red pulp. The liver had increased numbers of mononuclear cells within sinusoids and moderate Kupffer cell hyperplasia. In the heart of one infected mouse, the atrioventricular valves were mildly infiltrated by mononuclear inflammatory cells and edema (nonsuppurative valvular endocarditis).

EmCRT infection of mice and hamsters was confirmed postmortem through *in vitro* culture of the organism from cardiac blood and lung fluids, as well as by PCR of these fluids. Nearly all rodents tested during the acute phase of infection (9 to 14 dpi) displayed systemic dissemination of ehrlichiae to various organs (as evidenced by PCR/*in situ* hybridization [ISH]), including lungs, heart, liver, brain, kidneys, and spleen (Fig. 4; see also Fig. S2 in the supplemental material). Morulae were typically seen within 2 weeks in cultures inoculated with infected rodent blood, using either Giemsa stain and/or live fluorescence microscopy.

Tick infection. Naive *I. scapularis* larvae and nymphs that fed upon either infected hamsters or C57BL/6 mice successfully acquired EmCRT and, following molting, infected nymphs transmitted the bacteria to naive animals. Acquisition of ehrlichiae by ticks and successful transmission to rodents were demonstrated for both wild-type and transformed EmCRT. Transstadial retention of the bacteria was demonstrated by PCR in adults infected as either nymphs or larvae. These results were corroborated by confocal live microscopy, which identified fluorescent ehrlichiae in the synganglion, male accessory glands, acini of salivary glands (Fig. 5A), and the epithelial cells lining tracheae (Fig. 5B). Host-to-tick transmission success was very high (>90%) when ticks fed on infected rodents during a 24-h period immediately preceding PCR-confirmed bacteremia.

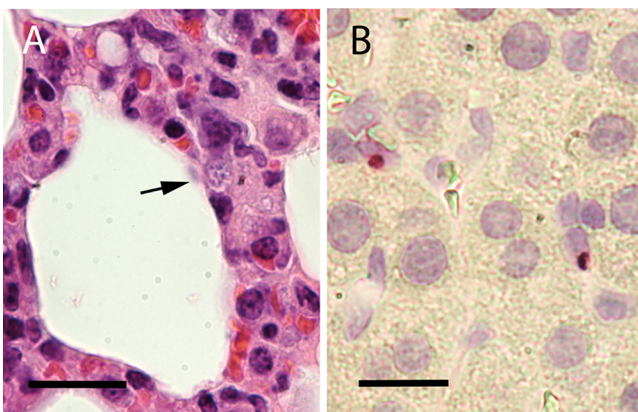


FIG 4 Lung tissue from a C57BL/6 mouse at 9 dpi. (A) H&E stain. The arrow indicates a morula near the alveolar space. (B) ISH assay performed on infected lung tissue. Red labeling indicates probe hybridization to ehrlichiae. Cell nuclei are stained light purple. Scale bars: 20 μm (A) and 10 μm (B).

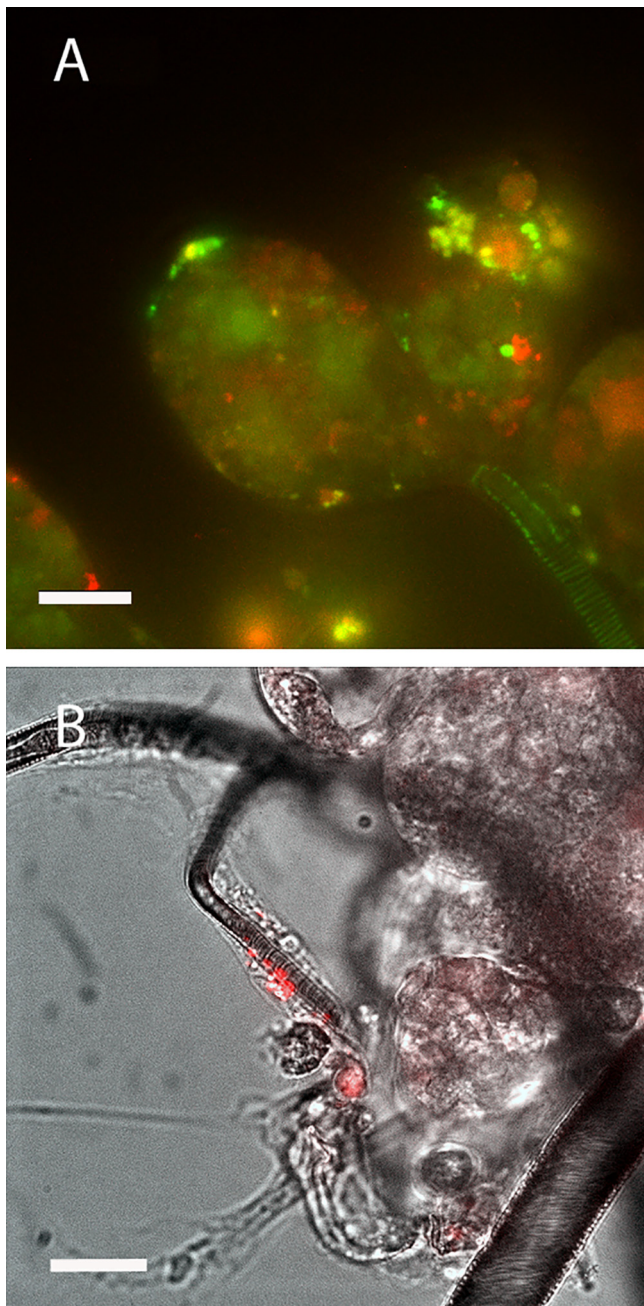


FIG 5 Live confocal images of tick tissues infected with mCherry EmCRT. (A) Salivary glands. Salivary ducts and acini are displayed. Red indicates EmCRT, and green and yellow indicate autofluorescence. (B) Tracheae. mCherry EmCRT is shown in red, superimposed over a bright-field image. Scale bars, 20 μm .

In contrast, 0 of the 9 nymphs from a group of approximately 100 lone star tick larvae that were allowed to feed on an EmCRT-infected hamster at 9 dpi acquired EmCRT. This included four individual nymphs and one pool of five nymphs, each of which tested negative by PCR for EmCRT after molting, despite a positive PCR result from the hamster blood collected immediately following tick repletion and detachment.

Of the field-collected *I. scapularis* we assessed from Camp Ripley, 1 of 26 (3.9%) female ticks collected in 2011, and 1 of 13 (7.7%) from 2012 tested positive by PCR, with *groESL* sequence matching *E. muris eauclairensis* and EmCRT.

Mutagenesis/detection/location. Five mCherry- and three mKate-expressing isolates were produced. Each of these mutants demonstrated the ability to grow in the

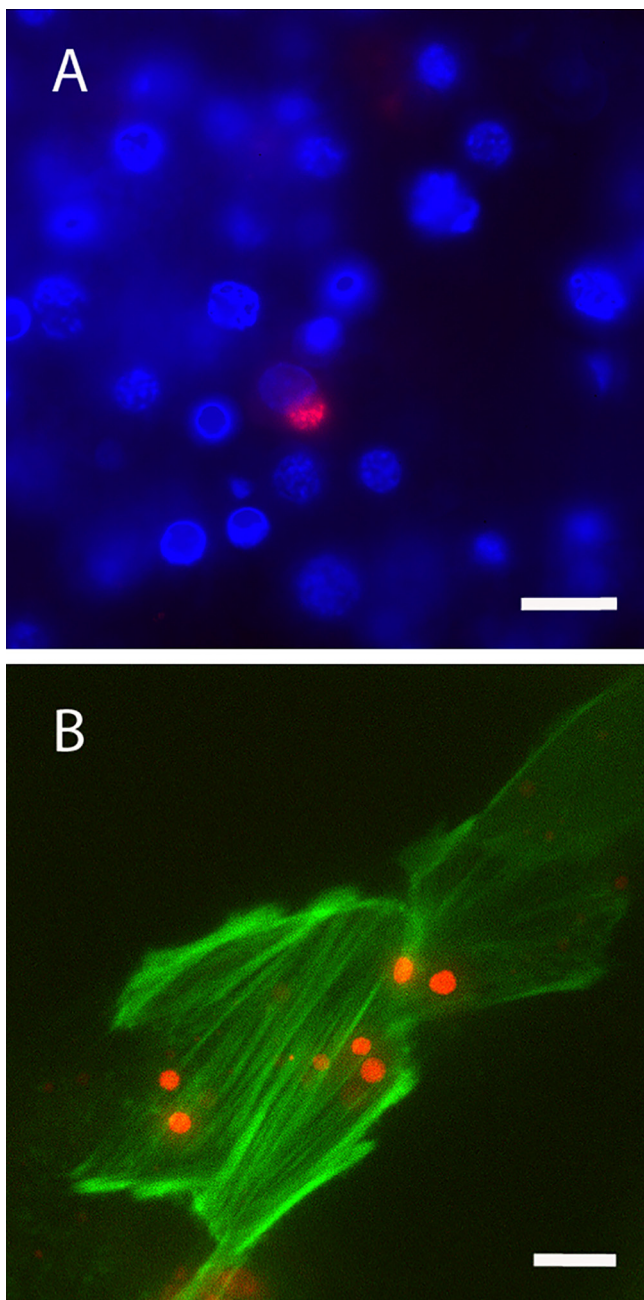


FIG 6 Live confocal images of mCherry EmCRT in culture. (A) EmCRT infecting ISE6 cells. Ehrlichiae are shown in red, and nuclei are stained blue with DAPI (4',6'-diamidino-2-phenylindole). (B) EmCRT infecting LifeAct RF/6A cells. Ehrlichiae are red, and host cell actin is green. Scale bars: 20 μm (A) and 10 μm (B).

ISE6 and RF/6A cell lines (Fig. 6). Expression of the mCherry and mKate proteins visible through live microscopy appeared to be stable for each isolate through 30 passages without antibiotic selection pressure. Transposon insertion sites were mapped for each mutant, revealing that two of eight isolates were comprised of a mixed mutant population (Table 1). Isolates D-69, 6/16, C5III, L27, and BUR contained intragenic insertions, while the B-65, 327, C5III, and EL isolates contained intergenic insertions. No obviously defective phenotype was observed for any isolate in either ISE6 cells or RF/6A cells.

Cell suspensions of mutants were inoculated into rodents via i.p. injection. Similar to wild-type EmCRT infection, bacteremia was detectable for mutants between 8 and

TABLE 1 Genomic insertion sites and proposed gene interruptions for mCherry and mKate EmCRT mutants generated using *Himar1* transposases^a

Isolate ID	Marker protein	Insertion site	Insertion site description	GenBank accession no.
D-69	mCherry	190757	EMU CRT_0888 hexapeptide transferase family protein	LANU01000003
B-65	mCherry	405998	Intergenic	LANU01000002
6/16	mCherry	256098	EMU CRT_0945 surface antigen family protein	LANU01000003
327	mKate	343269	Intergenic	LANU01000002
C5III#6	mKate	273221	Intergenic	LANU01000003
C5III#7	mKate	215557	EMU CRT_0175 exodeoxyribonuclease III	LANU01000001
L27	mKate	283891	EMU CRT_00523 hypothetical protein	LANU01000002
EL#6	mKate	209242	Intergenic	LANU01000002
EL#3	mKate	184916	Intergenic	LANU01000002
BUR	mKate	411816	EMU CRT_0644 hypothetical protein	LANU01000002

^aMixed isolates C5III and EL each contained two identifiable insertions. Accession numbers are listed for GenBank sequences containing each insertion site.

14 dpi and recoverable in cell culture, but in contrast to wild-type EmCRT, no morbidity and only a single mortality were observed in 25 hamsters and mice infected by either tick feeding or intraperitoneal (i.p.) inoculation. PCR was used to evaluate systemic infection with mutants, and the mCherry sequence was successfully amplified from all five tissues assessed (heart, lung, liver, spleen, and kidney) in at least one animal when two groups of three mice were infected with either the D-69 or B-65 mutants. This included positive lung samples from all six individuals assessed. A quantitative comparison of lung tissues between mice infected with either wild-type EmCRT or mCherry mutants indicated that the mean ehrlichial load in 10 ng of DNA from mouse lung tissue infected with wild-type EmCRT ($n = 49,766$) was not significantly different from the corresponding mean ($n = 16,410$) for lung tissue infected with mCherry mutant isolates ($2 \times P$ value < 0.299 ; Fig. S3). Larval *I. scapularis* ticks were allowed to feed on rodents infected with the D-69, B-65, 327, and EL isolates and assessed by PCR as nymphs for acquisition of mutant EmCRT. Each of the four isolates successfully colonized feeding larvae and were transstadially retained through the adult stage. All four mutants from the two mixed isolates were individually isolated in culture, and each of the EL mutants or wild-type *E. muris* was recovered in cell culture from hamster blood. However, there was no visual evidence of ehrlichiae in any of the four cultures inoculated with blood from hamsters infected with C5III mutants.

Transmission electron microscopy. Transmission electron microscopy (TEM) images of EmCRT-infected tick cells showed highly pleomorphic bacteria with a smooth inner and a corrugated outer membrane commonly seen in *Anaplasmataceae* (Fig. 7). The numbers of bacteria per cell and per morula were variable, and bacteria ranged in size from 0.25 to 1.5 μm . Cultured cells were fixed at an advanced stage of infection (>48 h postinoculation), where dense core and reticulate bodies could be seen within the same cell, and in some cases, within the same inclusion. Morulae containing mostly reticulate bodies tended to have fewer bacteria that were more tightly packed together, whereas dense core bodies were more widely spaced within morulae that contained a greater number of ehrlichiae. Cultured tick cells typically contained multiple morulae per cell at various stages of development, compared to hamster tissue cells that harbored single morulae containing a synchronous population of ehrlichiae. These observations were consistent with previously reported differences between ehrlichiae grown in tick cell culture and mammalian cell culture (26, 27). The morulae observed in tissues in this study had a similar general appearance to those in cell culture, but they were smaller and contained fewer bacteria than did the morulae in ISE6 cells. A fibrillar matrix, as reported for both RF/6A cells and mouse tissues infected with IOE (26, 28) and DH82 cells infected with *E. muris eauclairensis* sp. Wisconsin, was not observed in morulae in either of our *in vitro* or *in vivo* samples; however, vesicles were clearly visible within the morulae of ISE6 and tick tissues (Fig. 7C).

DISCUSSION

The EmCRT tick isolate as characterized here appears to be genotypically and phenotypically indistinguishable from the human-derived *E. muris eauclairensis* isolate,

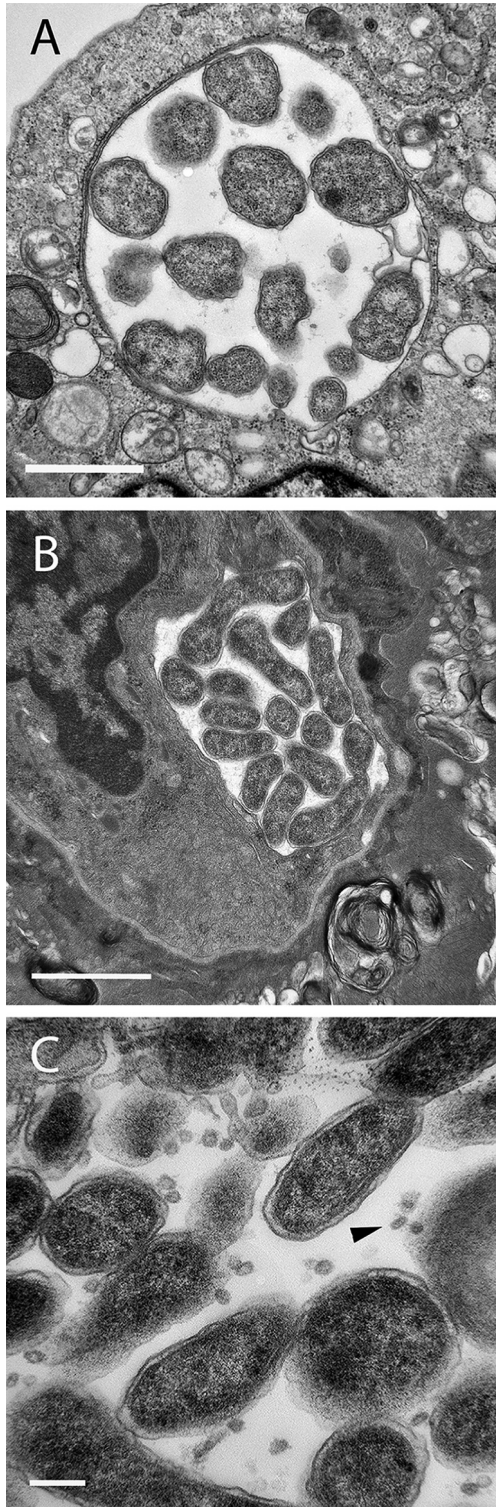


FIG 7 Electron micrographs of EmCRT. (A) Morula in ISE6 culture. (B) Morula in hamster lung tissue. (C) Ehrlichiae in the salivary gland of a female *I. scapularis*. The arrowhead points to vesicles of unknown origin. Scale bars: 1 μ m (A and B) and 200 nm (C).

Ehrlichia sp. Wisconsin. Sequences of the *groESL* operons from the two isolates were identical, although a more extensive comparison using multigene analysis would add further confidence. EmCRT has now been shown experimentally to infect lab mice, hamsters, and white-footed mice via tick challenge, reinforcing previous research

indicating that black-legged ticks are highly competent vectors and likely to be the source of most human ehrlichiosis cases caused by *E. muris eauclairensis*. Of additional epidemiologic importance, lone star ticks, a species established in states bordering Minnesota and Wisconsin and currently expanding its range, are not competent vectors of EmCRT, despite their ability to acquire and transmit other species of ehrlichial pathogens.

The demonstrated capacity of EmCRT to infect multiple types of cultured cell lines, as well as a wide range of tissues in live mammals and ticks (17, 21), suggests a broad cellular tropism. Similar to the human-derived *E. muris eauclairensis* and the *Ixodes ovatus Ehrlichia*, EmCRT infection was highly pathogenic for rodents, with systemic distribution of bacteria and disease often resulting in fatal acute respiratory distress syndrome. Consistent with previously reported fatal murine ehrlichiosis, histopathologic features of EmCRT infection were apparent in mouse livers and spleens and especially pronounced in the lungs (19, 28–31), which add to its utility as a model system for human monocytic ehrlichiosis (HME). As such, it is particularly applicable to reproducing acute respiratory distress syndrome, with findings in our study consistent with diffuse alveolar damage that included interstitial pneumonitis, pulmonary edema, and pulmonary hemorrhage. (32–36). Also consistent with HME and other pathogenic ehrlichioses, composite results of histology, ISH, and electron microscopy analysis of live mammalian rodent tissue performed in this study indicate that EmCRT infects a relatively small proportion of cells, which suggests that rather than cytopathic injury, pathogenesis is primarily a result of host immune response, leading to vascular leakage and toxic shock-like syndrome (30, 37, 38). These acute, severe disease outcomes contrast with the mild or asymptomatic, sublethal infections observed in laboratory mice infected with the type species isolate (*E. muris* AS145) obtained from a wild Japanese mouse, which may result in prolonged duration of infection (39, 40).

In our attempts to identify infected tissues in ticks, mutants were generated for the purpose of imaging EmCRT in live tissue, with some success. The autofluorescent features of tick anatomy we encountered reduced the ability to discern the mutants' marker protein in certain tissues, requiring careful dissection and use of samples of an appropriate thickness. Yet the images acquired using these mutants provided a foundation for further attempts at *in vivo* localization using molecular probes and electron microscopy (17). It is noteworthy, if not surprising, that none of our mutants showed a conspicuous phenotype in culture. This is likely because insertion events that disrupt critically important genes may result in nonviable, unrecoverable mutants, whereas those with intragenic insertions that are successfully recovered are likely those with redundant genes and/or alternate metabolic pathways. The observed reduction of virulence in rodent hosts, however, may have important immunological implications given that previous work using GFP- and mCherry-expressing mutant *Anaplasma marginale* has also shown reduced virulence compared to the wild type in cattle, despite also being phenotypically indistinguishable from the wild type in cell culture (41, 42). Moreover, while reduced virulence in mammalian hosts has previously been described for *E. chaffeensis* mutants with disruptions in critical genes (43, 44), our quantitative analysis did not show a statistically significant difference in ehrlichial load in mouse lung tissue infected with wild-type EmCRT compared to mutant-infected tissue. The reduced virulence phenotype could be caused by overexpression of mCherry and Spec from the transposon or, alternatively, the manipulation of the cultures associated with the transposon mutagenesis produced selective pressure, giving rise to spontaneous virulence attenuation mutants that are unrelated to the transposon insertion sites. Although the mechanism should be investigated, our results suggest that the reduction in rodent morbidity is more likely attributable to altered immunogenicity of the isolate than a reduction in viability. Among the four individual mutants originating from isolates with multiple insertions, it is unclear why neither of the C5III mutants were reisolated from hamsters.

While it appears that short duration of infection in hosts may be the primary factor responsible for low prevalence of *E. muris eauclairensis* in nature (19, 21, 45), its

relationship with coexistent *I. scapularis* transmitted pathogens, particularly *A. phagocytophilum* should also be examined. Antagonistic interaction between tick-borne pathogens has been described previously for *A. phagocytophilum* and other *Rickettsiaceae* (46, 47), and it is possible that inhibition or an alternate form of competition between *Anaplasmataceae* could significantly influence the relative distribution of these pathogens in natural ecosystems.

In conclusion, we document the second known culture isolate of *E. muris eaulclaiensis*, which as a human pathogen with a high degree of pathogenicity for rodents, is an ideal model organism for the study of acute HME. The creation of fluorescent protein-expressing EmCRT mutants will aid future genomic study of *E. muris*, as well as its interactions with hosts cells.

MATERIALS AND METHODS

Cultivation of Ehrlichia from infected tick organs. In October 2011, engorged ticks were collected from hunter-killed white-tailed deer (*Odocoileus virginianus*) at Camp Ripley, MN (46.094514°N, 94.3482°W), and an *Ehrlichia* sp. was isolated from one of the female *I. scapularis*. The tick was surface sterilized by 5-min sequential rinses in 0.1% sodium hypochlorite, 0.5% benzalkonium chloride, and 70% ethanol, followed by three rinses in purified water (EMD Millipore, Billerica, MA) (48). Then, 50 μ l of Tween 80 was added to 10 ml each of the bleach and benzalkonium chloride to enhance the wetting of tick surfaces. Ticks were submerged in \sim 50 μ l of L15C300 tick cell culture medium (supplemented as described below), whereupon the internal organs were extracted and introduced into wells of a 96-well plate seeded 3 days prior with the ISE6 cell line (ATCC CRL-11974; American Type Culture Collection [ATCC], Manassas, VA) derived from *I. scapularis* embryonic cells (49, 50). Cultures were incubated at 32°C in a humidified candle jar, grown in L15C300 medium supplemented with 10% fetal bovine serum (FBS; heat inactivated; Gemini Bio-Products, Sacramento, CA), 5% tryptose phosphate broth (Difco, Detroit, MI), 0.1% lipoprotein concentrate (MP Biomedical, Irvine, CA), and buffered with 25 mM HEPES and 0.25% NaHCO₃ (pH 7.6) (49, 50). Medium was replaced with fresh medium three times per week. The contents of wells that remained uncontaminated for 10 to 14 days were gently pipetted out of wells and transferred to larger wells (24-well plates seeded with ISE6 cells), where they were pooled with similar tissues from the same source tick. Once morulae (intracellular bacterium-containing vacuoles characteristic of *Anaplasmataceae*) were apparent, well contents were transferred by pipet into sealed 12.5-cm² flasks containing ISE6 cells and cultured at 34°C. Cultures were inspected for infection with intracellular bacteria by light microscopic examination of cell samples that had been centrifuged onto microscope slides, fixed in methanol, and stained in Giemsa solution. Microscopic identification was performed on a Nikon Eclipse 400 (Nikon, Melville, NY). The resulting isolate is referred to here as the *Ehrlichia muris*-like Camp Ripley tick (EmCRT) isolate.

Propagation of the ehrlichia isolate in cell culture. The EmCRT isolate was tested for its ability to infect five mammalian cell lines: the human promyelocytic leukemia cell line HL-60 (ATCC CRL-1780), the human monocytic leukemia cell line THP-1 (ATCC TIB-202), the human dermal microvascular endothelial cell line HMEC-1 (ATCC CRL-3243), the dog macrophage-like cell line DH82 (ATCC CRL 10389), and the rhesus (*Macaca mulatta*) endothelial cell line RF/6A (ATCC CRL-1780), either wild type or transformed with GFP-LifeAct to label the actin cytoskeleton for enhanced live microscopy detection (51). To obtain cell-free bacteria, ehrlichiae were first extracted from ISE6 cell suspension by vortexing at top speed with \sim 300 μ l of 60/90 sterile rock tumbler grit (Lortone, Mukilteo, WA). Grit was allowed to settle for 30 s, and the supernatant was passed through a 2- μ m-pore size Whatman polyvinylidene difluoride filter (GE Healthcare, Buckinghamshire, United Kingdom) onto a fresh cell layer or suspension of cells. Uninfected HMEC-1 and RF/6A cells, as well as infected and uninfected HL-60 and THP-1 cells, were cultured in RPMI 1640 medium with 25 mM HEPES buffer (Gibco, Carlsbad, CA), 2 mM L-glutamine (Gibco), and 10% FBS. DH82 cultures were grown using Dulbecco modified Eagle medium (Gibco), also with 2 mM L-glutamine and 10% FBS added. Infected HMEC-1, DH82, and RF/6A cells were cultured in supplemented L15C300 medium modified as described above and incubated at 37°C in a humidified atmosphere of 5% CO₂ in ambient air.

Giemsa-stained cell cultures were prepared and examined as described above. DNA was extracted with a Puregene blood core kit B (Qiagen Sciences, Gaithersburg, MD), and PCR was performed using GoTaq DNA polymerase (Promega, Madison, WI) with *Anaplasmataceae*-specific Per1 and Per2 primers under cycling conditions described previously (52) (Table 2). HS1 and HS6 primers were also used to amplify *groESL* sequence, using previously described cycling conditions (53). Amplicons (451- and 1,411-bp products) were visualized on a 1% agarose gel, and sequencing was performed at the University of Minnesota Genomics Center.

Phylogenetic analysis. *Ehrlichia groESL* operon sequences were obtained from GenBank to create an unrooted phylogenetic tree. The strains (accession numbers) used were as follows: *Ehrlichia ewingii* (AF195273.1), *Ehrlichia muris* AS145 (CP006917.1), *Ehrlichia muris* Nov Ip205 (GU358686.1), EmCRT (LANU01000002.1), *Ehrlichia* sp. strain Wisconsin (KU214846), *Ehrlichia* sp. strain HF (CP007474.1), "*Candidatus Ehrlichia ovata*" (IOE) (DQ672553.1), *Ehrlichia chaffeensis* strain Arkansas (CP000236.1), *Ehrlichia canis* strain Jake (CP000107.1), *Ehrlichia mineirensis* (CDGH01000062.1), "*Candidatus Ehrlichia khabarensis*" (KR063139.1), and *Ehrlichia ruminantium* (U13638.1).

TABLE 2 DNA oligonucleotides used in the study for PCR and probing, with target gene included when applicable

Primer	Direction	Sequence (5'–3')	Target
Per1	Forward	TTTATCGCTATTAGATGAGCCTATG	16S rDNA
Per2	Reverse	CTCTACACTAGGAATCCGCTAT	
HS1	Forward	TGGGCTGGTAATGAAAT	<i>groESL</i>
HS6	Reverse	CCICCGGIACIACACCTTC	
CherryF	Forward	TTGTTACGGTGACGCAGGATTC	Insertion
FR1	Forward	TTCTAACGGACCGGTTATGC	Insertion
SpecR	Reverse	GTTGTTTCATCAAGCCTTACGGTC	Insertion
Cherry up and out	Forward	ATTATCTTCTCTCCCTTGCTGACC	Insertion
Spec down and out	Reverse	CAGCCCGTCATACTTGAAGTAGGC	Insertion
EL#6 at 301339 ID F5	Forward	CTTGGTCCCCATACTGCTGG	Insertion
EL#6 at 301339 R	Reverse	AGCAACCGAACCATTGGGAT	Insertion
EL#3 at 325665 ID F	Forward	AGGAAGAGAGTGCTGATATGCA	Insertion
EL#3 at 325665 R	Reverse	CTTAGAGAACACAGGAAGCTGT	Insertion
C5III#6 at 1107523 ID F	Forward	ATCTGGCGGAGAAGTTGCTT	Insertion
C5III#6 at 1107523 R	Reverse	TTTGCTGGTCTGCTGTTGA	Insertion
C5III#7 at 625866 ID F	Forward	GGTGGAGATGCTAATTGGGGT	Insertion
C5III#7 at 625866 R	Reverse	CTGCAGCTTGTGGTGACAAC	Insertion

ClustalX 2.012 (54, 55) was used for sequence alignment, and maximum-likelihood trees were generated using MrBayes v.3.2.5 (56) with 1,000 bootstrap replicates and Phylogenerator (57). Each program was used under default parameters and produced trees that agreed with each other. FigTree v1.4.2 (58) and Adobe Photoshop were used for additional modification of the final tree included here.

Rodent infection and histology. All animals in this study were maintained and used under a protocol approved by the University of Minnesota Institutional Animal Care and Use Committee (1307-30753A) in accordance with recommendations listed in the *Guide for the Care and Use of Laboratory Animals* of the National Institutes of Health (59). Female C57BL/6 mice ranging from 4 to 12 weeks old and outbred Syrian hamsters (*Mesocricetus auratus*) of either sex ranging from 4 to 8 weeks old were infected i.p. by injection of 300 to 500 μ l of an *Ehrlichia*-infected cell suspension, estimated by Giemsa stain and hemocytometer to contain 3×10^5 infected cells. Animals were euthanized at 8 to 12 dpi, and blood was drawn postmortem via cardiac puncture for DNA extraction using the Puregene blood core kit B. Bacterial DNA was then amplified by PCR targeting 16S ribosomal DNA (rDNA) and *groESL* regions (see below and Table 2) and sequenced at the University of Minnesota Genomics Center.

In addition to PCR, blood (100 to 500 μ l) from infected animals was inoculated onto ISE6 cells to reisolate the pathogen and confirm current infection. Sterile 15% EDTA solution (Na_2 salt; Kendall/Covidien, Mansfield, MA) was used to prevent hamster blood from clotting. Cells were cultured and assessed for infection via PCR and Giemsa staining as described above.

Rodents were dissected immediately following euthanasia, and organs fixed in a 10% buffered formalin solution for 24 to 48 h at 4°C, followed by storage in 70% ethanol. Fixed tissues were paraffin embedded and sectioned at 4 μ m onto slides (Fisher Scientific, Hampton, NH), and a subset was stained with hematoxylin and eosin (H&E) at the Masonic Cancer Center Comparative Pathology Laboratory at the University of Minnesota. Unstained paraffin-embedded lung sections were processed using ISH, as previously described (21). Unfixed samples of the organs for PCR analysis were also collected and frozen at –70°C prior to extraction of DNA using a DNeasy blood and tissue kit (Qiagen). PCR assays used 100 ng of template DNA extracted from 10- to 20-mg pieces of tissue.

Tick infection. Gravid specific-pathogen-free *I. scapularis* and lone star ticks (*Amblyomma americanum*) were obtained from a colony maintained at Oklahoma State University (Stillwater, OK) and stored at room temperature under 97% humidity and a 16:8-h light-dark cycle, where they proceeded to oviposit. Larvae were fed to repletion on mice or hamsters and then washed in 0.1% bleach solution, rinsed with Milli-Q filtered water, and housed in vented 5-ml polystyrene tubes (BD Biosciences, Canaan, CT) stored in a desiccator over a saturated solution of K_2SO_4 . When needle inoculation was used to infect hosts, approximately 50 larvae were placed on each animal at 8 to 10 dpi, and only ticks that engorged were collected. For hosts infected via ticks, naive larvae were placed 10 or 11 days after the initiation of nymphal feeding. After molting, a subset of ticks was washed in 0.1% bleach, rinsed twice in Milli-Q filtered water, and bisected with a sterile needle in a 1.5-ml microcentrifuge tube. Tissue was denatured for at least 24 h in cell lysis buffer prior to DNA extraction using the Puregene kit. A pooled sample consisted of five nymphs processed simultaneously. Adult *I. scapularis* ticks were obtained by feeding nymphs on either hamsters or mice at densities of 10 to 20 ticks per animal. Additional engorged female ticks collected from Camp Ripley deer in 2011 and 2012 were cleaned, cultured, and evaluated for ehrlichial infection as described above.

Mutagenesis/detection/location. EmCRT was transformed using the *Himar1* transposase system as described in Felsheim et al. (60). Two plasmid constructs (pCis mCherry-SS *Himar1* A7 and pCis mKate-SS *Himar1* A7) each encoding both the transposase and the transposon, were used for transformation, with either mCherry or mKate as the fluorescent marker (see Fig. S1 in the supplemental material) (43). Modification of the above protocol included use of sterile Lortone grit to lyse infected cells and the centrifugation of bacteria with ISE6 cells at $5,000 \times g$ for 5 min following electroporation. Bacterial/cell

pellets were allowed to sit at room temperature for 30 min prior to being resuspended and added to ISE6 cell cultures in 25-cm² flasks. Starting 2 to 3 days after electroporation, transformants were selected using 0.25 mg each of spectinomycin (5 μ l of 50 mg/ml solution) and streptomycin (25 μ l of 10 mg/ml solution) per 5 ml of medium (60, 61).

To confirm the insertion of the expression cassettes into the EmCRT genome, PCR was performed on DNA extracted from the mutant EmCRT-infected cultures using the Puregene blood core kit A with GoTaq DNA polymerase and one of two primer sets: (i) CherryF and SpecR targeting transposon gene sequences in mCherry-expressing mutants or (ii) FR1 and SpecR targeting sequences expressing mKate (Table 2). Cycling conditions were as follows: 95°C for 2 min for one cycle; 95°C for 30 s, 55°C for 30 s, and 72°C for 1 min for 35 cycles; followed by a final extension at 72°C for 5 min. Amplicons were electrophoresed on a 1% agarose gel and stained with GelGreen (Biotium, Inc., Hayward, CA) for visualization.

Southern analysis was performed as previously described by Baldrige et al. (62) using 500 ng of BglII-digested DNA per mutant EmCRT isolate and hybridization with a digoxigenin-labeled Spec probe at 65°C. Integration sites were then identified by plasmid rescue cloning. Briefly, EcoRI- or HindIII-cut genomic EmCRT DNA was ligated to pGEM (Promega) overnight at 14°C, electroporated into DH5 α -E competent cells (Invitrogen), and plated onto YT agar plates containing 50 μ g/ml each of streptomycin and spectinomycin, as well as 75 μ g/ml ampicillin. Bacteria from individual colonies were grown in tubes containing Terrific broth, and plasmid DNA was extracted using a High Pure plasmid isolation kit (Roche) in accordance with the manufacturer's protocol. All sequencing was performed at the University of Minnesota Genomics Center using the primers Cherry up and out and Spec down and out (Table 2). Clones representing each of the four known transposon insertions found in the two mixed mKate isolates were isolated by serial 2-fold dilution where cell-free suspensions of ehrlichiae were inoculated onto 96-well plates seeded with ISE6 cells. Cultures of ISE6 cells infected with mixed mutants were adjusted to 100 infected cells/ml (infection percentage determined with Giemsa-stained cytospin preparations) and, using a multichannel pipettor, 100 μ l was diluted from left to right across 96-well plates containing light (~70% confluent) monolayers of ISE6 cells with 100 μ l of medium/well. Plates were incubated at 34°C in a 4% CO₂, water-saturated atmosphere for 7 days, and then 200 μ l/well of additional medium was added to plates right to left. On day 18, the last infected well in each row was identified by visualizing the mutants' characteristic red fluorescence using an inverted microscope with UV illumination. These wells were harvested for DNA extraction and PCR analysis was used to determine which contained pure mutants, as described below. The contents of wells containing pure mutants were subcultured into a 24-well plate, and once the cultures reached maturity, frozen stocks were made. Primer sets specific for each EL or C5III insertion site were used (Table 2). Clonal isolates were transferred to fresh ISE6 cultures and, when fully infected, 200 μ l of cell suspension of each clonal mutant was injected separately into one male and one female 4-week-old hamster originating from a single litter. At 7 dpi, the hamsters were euthanized by using CO₂ overexposure, blood was drawn via cardiac puncture, and HL60 and ISE6 cultures were inoculated with 150 μ l of blood. Cultures were checked daily for ehrlichiae using fluorescence microscopy and intermittently by examination of Giemsa-stained cells for 25 days.

Quantitative PCR (qPCR) was used to determine the quantities of wild-type and transformed EmCRT in mouse lung tissue. Quantitative PCR was performed as previously described (63) using an Mx3005 qPCR cycler (Stratagene), Brilliant II SYBR green qPCR master mix (Stratagene), a 240 nM concentration of each primer, 100 ng of mouse lung tissue DNA, and serial dilutions of plasmid DNA adjusted to 10 ng of DNA per sample with salmon sperm DNA (Promega). Primers that target the single-copy 16S rRNA gene in EmCRT [PER5(20) and PER6-EmCRT (5'-CCTTCATGTCAAAAAGTGGTAAGG-3')] were used, and a standard curve was generated using a plasmid created by PCR amplification of EmCRT with the 16S rRNA primers PER4(20) and PER6-EmCRT. The cycling parameters were 1 cycle at 95°C for 10 min; 40 cycles at 95°C for 30 s, 59°C for 1 min, and 72°C for 30 s; with a dissociation curve cycle of 95°C for 1 min, 58°C for 30 s, and 95°C for 30 s to confirm product specificity. MxPro v4 software was used to acquire the data and to reference genomic sample values to the standard curve. Values were expressed as an average of amplification from samples run in triplicate on one plate.

Transmission electron microscopy. Cultures of *Ehrlichia*-infected ISE6 cells were gently washed off the culture flask using a stream of medium, pelleted by centrifugation at 300 \times g for 5 min, and rinsed twice with PBS. Pellets were then fixed overnight at 4°C using a modified Ito fixative (64, 65). Hamster lung tissue was collected at 9 dpi and immediately fixed overnight at 4°C, as were whole adult female *I. scapularis* using Ito fixative. The dehydration, staining, and embedding procedures for the cells and tissues were performed as described by Lynn et al. (17).

Imaging. Confocal images were taken using a Quantem:512SC electron multiplying charge-coupled-device camera (Photometrics, Tucson, AZ) interfaced with a BX61 DSU spinning disk confocal microscope (Olympus America, Center Valley, PA) equipped with an X-cite Exacte fluorescent light source (Lumen Dynamics, Mississauga, Ontario, Canada). An Olympus Q-Fire digital camera was used to image slides stained with Giemsa or processed using ISH. MetaMorph Premier (Molecular Devices, Sunnyvale, CA) imaging software in conjunction with ImageJ software (National Institutes of Health, Bethesda, MD) was used to acquire and process images. In addition, some Giemsa-stained cell samples were viewed and imaged using a Nikon Eclipse 400 microscope equipped with a Nikon DXM 1200 digital camera controlled by ACT-1 imaging software (Nikon). Adjustments to improve color balance and sharpness were made using Adobe Photoshop. Histological images were taken with Spot Insight 4.0 Megapixel color mosaic camera using Spot v5.2 imaging software. Contrast, brightness, and sharpness were adjusted linearly across the whole image in Adobe Photoshop.

SUPPLEMENTAL MATERIAL

Supplemental material for this article may be found at <https://doi.org/10.1128/AEM.00866-19>.

SUPPLEMENTAL FILE 1, PDF file, 0.8 MB.

ACKNOWLEDGMENTS

We thank Lisa Price for contributing PCR sequences for Camp Ripley ticks, the University of Minnesota Imaging Centers for sectioning and staining samples for TEM and assistance with microscope operation, and Mike Herron for contributing GFP-expressing LifeAct RF/6A cells.

The study was funded under grant R01AI042792 provided by the National Institutes of Health (USA) and awarded to U.G.M. The funders had no role in study design, data collection and analysis, decision to publish, or preparation of the manuscript.

REFERENCES

- Robinson SJ, Neitzel DF, Moe RA, Craft ME, Hamilton KE, Johnson LB, Mulla DJ, Munderloh UG, Redig PT, Smith KE, Turner CL, Umber JK, Pelican KM. 2015. Disease risk in a dynamic environment: the spread of tick-borne pathogens in Minnesota, USA. *Ecohealth* 12:152–163. <https://doi.org/10.1007/s10393-014-0979-y>.
- Eisen RJ, Kugeler KJ, Eisen L, Beard CB, Paddock CD. 2017. Tick-borne zoonoses in the United States: persistent and emerging threats to human health. *ILAR J* 58:319–335. <https://doi.org/10.1093/ilar/ilx005>.
- Eisen RJ, Eisen L. 2018. The blacklegged tick, *Ixodes scapularis*: an increasing public health concern. *Trends Parasitol* 34:295–309. <https://doi.org/10.1016/j.pt.2017.12.006>.
- Mead PS. 2015. Epidemiology of Lyme disease. *Infect Dis Clin North Am* 29:187–210. <https://doi.org/10.1016/j.idc.2015.02.010>.
- Bakken JS, Dumler JS, Chen SM, Eckman MR, Van Etta LL, Walker DH. 1994. Human granulocytic ehrlichiosis in the upper Midwest United States: a new species emerging? *JAMA* 272:212–218. <https://doi.org/10.1001/jama.1994.03520030054028>.
- Chen SM, Dumler JS, Bakken JS, Walker DH. 1994. Identification of a granulocytotropic *Ehrlichia* species as the etiologic agent of human disease. *J Clin Microbiol* 32:589–595.
- Neitzel DF, Kemperman MM. 2012. Tick-borne diseases in Minnesota: an update. *Minn Med* 95:41–44.
- Wisconsin Department of Health Services. 2019. Anaplasmosis and ehrlichiosis. Wisconsin Department of Health Services, Madison, WI. <https://www.dhs.wisconsin.gov/tickborne/ae/index.htm>. Accessed 10 February 2019.
- Pritt BS, Respcio-Kingry LB, Sloan LM, Schriefer ME, Replogle AJ, Bjork J, Liu G, Kingry LC, Mead PS, Neitzel DF, Schiffman E, Hoang Johnson DK, Davis JP, Paskewitz SM, Boxrud D, Deedon A, Lee X, Miller TK, Feist MA, Steward CR, Theel ES, Patel R, Irish CL, Petersen JM. 2016. *Borrelia mayonii* sp. nov., a member of the *Borrelia burgdorferi* sensu lato complex, detected in patients and ticks in the upper midwestern United States. *Int J Syst Evol Microbiol* 66:4878–4880. <https://doi.org/10.1099/ijsem.0.001445>.
- Pritt BS, Sloan LM, Johnson DKH, Munderloh UG, Paskewitz SM, McElroy KM, McFadden JD, Binnicker MJ, Neitzel DF, Liu G, Nicholson WL, Nelson CM, Franson JJ, Martin SA, Cunningham SA, Steward CR, Bogumill K, Bjorgaard ME, Davis JP, McQuiston JH, Warshauer DM, Wilhelm MP, Patel R, Trivedi VA, Ereemeeva ME. 2011. Emergence of a new pathogenic *Ehrlichia* species, Wisconsin and Minnesota, 2009. *N Engl J Med* 365:422–429. <https://doi.org/10.1056/NEJMoa1010493>.
- Pritt BS, Allerdice MEJ, Sloan LM, Paddock CD, Munderloh UG, Rikihisa Y, Tajima T, Paskewitz SM, Neitzel DF, Hoang Johnson DK, Schiffman E, Davis JP, Goldsmith CS, Nelson CM, Karpathy SE. 2017. Proposal to reclassify *Ehrlichia muris* as *Ehrlichia muris* subsp. *muris* subsp. nov. and description of *Ehrlichia muris* subsp. *eaucalarensis* subsp. nov., a newly recognized tick-borne pathogen of humans. *Int J Syst Evol Microbiol* 67:2121–2126. <https://doi.org/10.1099/ijsem.0.001896>.
- Comer JA, Nicholson WL, Olson JG, Childs JE. 1999. Serologic testing for human granulocytic ehrlichiosis at a national referral center. *J Clin Microbiol* 37:558–564.
- Centers for Disease Control and Prevention. 2019. Ehrlichiosis: clinical and laboratory diagnosis. Centers for Disease Control and Prevention, Atlanta, GA. <https://www.cdc.gov/ehrlichiosis/healthcare-providers/diagnosis.html>.
- Xu G, Pearson P, Rich SM. 2018. *Ehrlichia muris* in *Ixodes cookei* ticks, northeastern United States, 2016–2017. *Emerg Infect Dis* 24:1143–1144. <https://doi.org/10.3201/eid2406.171755>.
- Telford Iii SR, Goethert HK, Cunningham JA. 2011. Prevalence of *Ehrlichia muris* in Wisconsin deer ticks collected during the mid-1990s. *Open Microbiol J* 5:18–20. <https://doi.org/10.2174/1874285801105010018>.
- Stromdahl E, Hamer S, Jenkins S, Sloan L, Williamson P, Foster E, Nadolny R, Elkins C, Vince M, Pritt B. 2014. Comparison of phenology and pathogen prevalence, including infection with the *Ehrlichia muris*-like (EML) agent, of *Ixodes scapularis* removed from soldiers in the midwestern and the northeastern United States over a 15-year period (1997–2012). *Parasit Vectors* 7:553. <https://doi.org/10.1186/PREACCEPT-1577044381141706>.
- Lynn GE, Oliver JD, Nelson CM, Felsheim RF, Kurtti TJ, Munderloh UG. 2015. Tissue distribution of the *Ehrlichia muris*-like agent in a tick vector. *PLoS One* 10:e0122007. <https://doi.org/10.1371/journal.pone.0122007>.
- Saito TB, Walker DH. 2015. A tick vector transmission model of monocytotropic ehrlichiosis. *J Infect Dis* 212:968–977. <https://doi.org/10.1093/infdis/jiv134>.
- Karpathy SE, Allerdice MEJ, Sheth M, Dasch GA, Levin ML. 2016. Co-feeding transmission of the *Ehrlichia muris*-like agent to mice (*Mus musculus*). *Vector Borne Zoonotic Dis* 16:145–150. <https://doi.org/10.1089/vbz.2015.1878>.
- Castillo CG, Ereemeeva ME, Paskewitz SM, Sloan LM, Lee X, Irwin WE, Tonsberg S, Pritt BS. 2015. Detection of human pathogenic *Ehrlichia muris*-like agent in *Peromyscus leucopus*. *Ticks Tick Borne Dis* 6:155–157. <https://doi.org/10.1016/j.ttbdis.2014.11.006>.
- Lynn GE, Oliver JD, Cornax I, O'Sullivan MG, Munderloh UG. 2017. Experimental evaluation of *Peromyscus leucopus* as a reservoir host of the *Ehrlichia muris*-like agent. *Parasit Vectors* 10:48. <https://doi.org/10.1186/s13071-017-1980-4>.
- Heimer R, Tisdale D, Dawson J. 1998. A single tissue culture system for the propagation of the agents of the human ehrlichioses. *Am J Trop Med Hyg* 58:812–815. <https://doi.org/10.4269/ajtmh.1998.58.812>.
- Barnewall RE, Rikihisa Y, Lee EH. 1997. *Ehrlichia chaffeensis* inclusions are early endosomes which selectively accumulate transferrin receptor. *Infect Immun* 65:1455–1461.
- Dawson JE, Anderson BE, Fishbein DB, Sanchez JL, Goldsmith CS, Wilson KH, Duntley CW. 1991. Isolation and characterization of an *Ehrlichia* sp. from a patient diagnosed with human ehrlichiosis. *J Clin Microbiol* 29:2741–2745.
- Dawson JE, Candal FJ, George VG, Ades EW. 1993. Human endothelial cells as an alternative to DH82 cells for isolation of *Ehrlichia chaffeensis*, *E. canis*, and *Rickettsia rickettsii*. *Pathobiology* 61:293–296. <https://doi.org/10.1159/000163808>.
- Munderloh UG, Silverman DJ, MacNamara KC, Ahlstrand GG, Chatterjee M, Winslow GM. 2009. *Ixodes ovatus Ehrlichia* exhibits unique ultrastructural characteristics in mammalian endothelial and tick-derived cells. *Ann N Y Acad Sci* 1166:112–119. <https://doi.org/10.1111/j.1749-6632.2009.04520.x>.
- Dedonder SE, Cheng C, Willard LH, Boyle DL, Ganta RR. 2012. Transmission electron microscopy reveals distinct macrophage- and tick cell-

- specific morphological stages of *Ehrlichia chaffeensis*. PLoS One 7:e36749. <https://doi.org/10.1371/journal.pone.0036749>.
28. Sotomayor EA, Popov VL, Feng HM, Walker DH, Olano JP. 2001. Animal model of fatal human monocytotropic ehrlichiosis. Am J Pathol 158: 757–769. [https://doi.org/10.1016/S0002-9440\(10\)64018-7](https://doi.org/10.1016/S0002-9440(10)64018-7).
 29. Shibata S, Kawahara M, Rikihisa Y, Fujita H, Watanabe Y, Suto C, Ito T. 2000. New *Ehrlichia* species closely related to *Ehrlichia chaffeensis* isolated from *Ixodes ovatus* ticks in Japan. J Clin Microbiol 38:1331–1338.
 30. Ismail N, Soong L, McBride JW, Valbuena G, Olano JP, Feng H-M, Walker DH. 2004. Overproduction of TNF- α by CD8⁺ type 1 cells and down-regulation of IFN- γ production by CD4⁺ Th1 cells contribute to toxic shock-like syndrome in an animal model of fatal monocytotropic ehrlichiosis. J Immunol 172:1786–1800. <https://doi.org/10.4049/jimmunol.172.3.1786>.
 31. Saito TB, Thirumalapura NR, Shelite TR, Rockx-Brouwer D, Popov VL, Walker DH. 2015. An animal model of a newly emerging human ehrlichiosis. J Infect Dis 211:452–461. <https://doi.org/10.1093/infdis/jiu372>.
 32. Wong S, Grady LJ. 1996. *Ehrlichia* infection as a cause of severe respiratory distress. N Engl J Med 334:273. <https://doi.org/10.1056/NEJM199601253340418>.
 33. Fichtenbaum CJ, Peterson LR, Weil GJ. 1993. Ehrlichiosis presenting as a life-threatening illness with features of the toxic shock syndrome. Am J Med 95:351–357. [https://doi.org/10.1016/0002-9343\(93\)90302-6](https://doi.org/10.1016/0002-9343(93)90302-6).
 34. Marty AM, Dumler JS, Imes G, Brusman HP, Smrkovski LL, Frisman DM. 1995. Ehrlichiosis mimicking thrombotic thrombocytopenic purpura: case report and pathological correlation. Hum Pathol 26:920–925. [https://doi.org/10.1016/0046-8177\(95\)90017-9](https://doi.org/10.1016/0046-8177(95)90017-9).
 35. Sehdev AE, Dumler JS. 2003. Hepatic pathology in human monocytic ehrlichiosis: *Ehrlichia chaffeensis* infection. Am J Clin Pathol 119: 859–865. <https://doi.org/10.1309/F7EA-B5P7-3217-16LJ>.
 36. Dawson JE, Paddock CD, Warner CK, Greer PW, Bartlett JH, Ewing SA, Munderloh UG, Zaki SR. 2001. Tissue diagnosis of *Ehrlichia chaffeensis* in patients with fatal ehrlichiosis by use of immunohistochemistry, *in situ* hybridization, and polymerase chain reaction. Am J Trop Med Hyg 65:603–609. <https://doi.org/10.4269/ajtmh.2001.65.603>.
 37. Dumler JS, Dawson JE, Walker DH. 1993. Human ehrlichiosis: hematopathology and immunohistologic detection of *Ehrlichia chaffeensis*. Hum Pathol 24:391–396. [https://doi.org/10.1016/0046-8177\(93\)90087-W](https://doi.org/10.1016/0046-8177(93)90087-W).
 38. Walker DH, Dumler JS. 1997. Human monocytic and granulocytic ehrlichioses. Discovery and diagnosis of emerging tick-borne infections and the critical role of the pathologist. Arch Pathol Lab Med 121:785–791.
 39. Kawahara M, Suto C, Rikihisa Y, Yamamoto S, Tsuboi Y. 1993. Characterization of ehrlichial organisms isolated from a wild mouse. J Clin Microbiol 31:89–96.
 40. Olano JP, Wen G, Feng H-M, McBride JW, Walker DH. 2004. Histologic, serologic, and molecular analysis of persistent ehrlichiosis in a murine model. Am J Pathol 165:997–1006. [https://doi.org/10.1016/S0002-9440\(10\)63361-5](https://doi.org/10.1016/S0002-9440(10)63361-5).
 41. Hammac GK, Ku P-S, Galletti MF, Noh SM, Scoles GA, Palmer GH, Brayton KA. 2013. Protective immunity induced by immunization with a live, cultured *Anaplasma marginale* strain. Vaccine 31:3617–3622. <https://doi.org/10.1016/j.vaccine.2013.04.069>.
 42. Crosby FL, Brayton KA, Magunda F, Munderloh UG, Kelley KL, Barbet AF. 2015. Reduced infectivity in cattle for an outer membrane protein mutant of *Anaplasma marginale*. Appl Environ Microbiol 81:2206–2214. <https://doi.org/10.1128/AEM.03241-14>.
 43. Cheng C, Nair ADS, Indukuri VV, Gong S, Felsheim RF, Jaworski D, Munderloh UG, Ganta RR. 2013. Targeted and random mutagenesis of *Ehrlichia chaffeensis* for the identification of genes required for *in vivo* infection. PLoS Pathog 9:e1003171. <https://doi.org/10.1371/journal.ppat.1003171>.
 44. Cheng C, Nair ADS, Jaworski DC, Ganta RR. 2015. Mutations in *Ehrlichia chaffeensis* causing polar effects in gene expression and differential host specificities. PLoS One 10:e0132657. <https://doi.org/10.1371/journal.pone.0132657>.
 45. Johnson TJ, Graham CB, Maes SE, Hojgaard A, Fleshman A, Boegler KA, Delory MJ, Slater KS, Karpathy SE, Bjork JK, Neitzel DF, Schiffman EK, Eisen RJ. 2018. Prevalence and distribution of seven pathogens in host-seeking *Ixodes scapularis* (Acari: Ixodidae) nymphs in Minnesota, USA. Ticks Tick Borne Dis 9:1499–1507. <https://doi.org/10.1016/j.ttbdis.2018.07.009>.
 46. Levin ML, Fish D. 2001. Interference between the agents of Lyme disease and human granulocytic ehrlichiosis in a natural reservoir host. Vector Borne Zoonotic Dis 1:139–148. <https://doi.org/10.1089/153036601316977741>.
 47. Macaluso KR, Sonenshine DE, Ceraul SM, Azad AF. 2002. Rickettsial infection in *Dermacentor variabilis* (Acari: Ixodidae) inhibits transovarial transmission of a second *Rickettsia*. J Med Entomol 39:809–813. <https://doi.org/10.1603/0022-2585-39.6.809>.
 48. Kurtti TJ, Munderloh UG, Hughes CA, Engstrom SM, Johnson RC. 1996. Resistance to tick-borne spirochete challenge induced by *Borrelia burgdorferi* strains that differ in expression of outer surface proteins. Infect Immun 64:4148–4153.
 49. Munderloh UG, Jauron SD, Fingerle V, Leitritz L, Hayes SF, Hautman JM, Nelson CM, Huberty BW, Kurtti TJ, Ahlstrand GG, Greig B, Mellencamp MA, Goodman JL. 1999. Invasion and intracellular development of the human granulocytic ehrlichiosis agent in tick cell culture. J Clin Microbiol 37:2518–2524.
 50. Oliver JW, Burkhardt NY, Felsheim RF, Kurtti TJ, Munderloh UG. 2014. Motility characteristics are altered for *Rickettsia bellii* transformed to overexpress a heterologous *rickA* gene. Appl Environ Microbiol 80: 1170–1176. <https://doi.org/10.1128/AEM.03352-13>.
 51. Riedl J, Crevenna AH, Kessenbrock K, Yu JH, Neukirchen D, Bista M, Bradke F, Jenne D, Holak TA, Werb Z, Sixt M, Wedlich-Soldner R. 2008. LifeAct: a versatile marker to visualize F-actin. Nat Methods 5:605–607. <https://doi.org/10.1038/nmeth.1220>.
 52. Goodman JL, Nelson C, Vitale B, Madigan JE, Dumler JS, Kurtti TJ, Munderloh UG. 1996. Direct cultivation of the causative agent of human granulocytic ehrlichiosis. N Engl J Med 334:209–215. <https://doi.org/10.1056/NEJM199601253340401>.
 53. Sumner JW, Nicholson WL, Massung RF. 1997. PCR amplification and comparison of nucleotide sequences from the *groESL* heat shock operon of *Ehrlichia* species. J Clin Microbiol 35:2087–2092.
 54. Larkin MA, Blackshields G, Brown NP, Chenna R, McGettigan PA, McWilliam H, Valentin F, Wallace IM, Wilm A, Lopez R, Thompson JD, Gibson TJ, Higgins DG. 2007. ClustalW and ClustalX version 2.0. Bioinformatics 23:2947–2948. <https://doi.org/10.1093/bioinformatics/btm404>.
 55. Goujon M, McWilliam H, Li W, Valentin F, Squizzato S, Paern J, Lopez R. 2010. A new bioinformatics analysis tools framework at EMBL-EBI. Nucleic Acids Res 38:W695–W699. <https://doi.org/10.1093/nar/gkq313>.
 56. Ronquist F, Teslenko M, van der Mark P, Ayres DL, Darling A, Höhna S, Larget B, Liu L, Suchard MA, Huelsenbeck JP. 2012. MrBayes 3.2: efficient Bayesian phylogenetic inference and model choice across a large model space. Syst Biol 61:539–542. <https://doi.org/10.1093/sysbio/sys029>.
 57. Pearse WD, Purvis A. 2013. phyloGenerator: an automated phylogeny generation tool for ecologists. Methods Ecol Evol 4:692–698. <https://doi.org/10.1111/2041-210X.12055>.
 58. Rambaut A. 2015. FigTree v1.4.2. <http://tree.bio.ed.ac.uk/software/figtree/>.
 59. National Institutes of Health. 2011. Guide for the care and use of laboratory animals, 8th ed. National Institutes of Health, Bethesda, MD. <https://www.ncbi.nlm.nih.gov/books/NBK54050/>. Accessed 21 January 2016.
 60. Felsheim RF, Herron MJ, Nelson CM, Burkhardt NY, Barbet AF, Kurtti TJ, Munderloh UG. 2006. Transformation of *Anaplasma phagocytophilum*. BMC Biotechnol 6:42. <https://doi.org/10.1186/1472-6750-6-42>.
 61. Shaner NC, Campbell RE, Steinbach PA, Giepmans BNG, Palmer AE, Tsien RY. 2004. Improved monomeric red, orange and yellow fluorescent proteins derived from *Discosoma* sp. red fluorescent protein. Nat Biotechnol 22:1567–1572. <https://doi.org/10.1038/nbt1037>.
 62. Baldrige GD, Burkhardt N, Herron MJ, Kurtti TJ, Munderloh UG. 2005. Analysis of fluorescent protein expression in transformants of *Rickettsia monacensis*, an obligate intracellular tick symbiont. Appl Environ Microbiol 71:2095–2105. <https://doi.org/10.1128/AEM.71.4.2095-2105.2005>.
 63. Baldrige GD, Burkhardt NY, Labruna MB, Pacheco RC, Paddock CD, Williamson PC, Billingsley PM, Felsheim RF, Kurtti TJ, Munderloh UG. 2010. Wide dispersal and possible multiple origins of low-copy-number plasmids in rickettsia species associated with blood-feeding arthropods. Appl Environ Microbiol 76:1718–1731. <https://doi.org/10.1128/AEM.02988-09>.
 64. Ito S, Vinson JW, McGuire TJ. 1975. Murine typhus *Rickettsiae* in the Oriental rat flea. Ann N Y Acad Sci 266:35–60. <https://doi.org/10.1111/j.1749-6632.1975.tb35087.x>.
 65. Kurtti TJ, Munderloh UG, Hayes SF, Krueger DE, Ahlstrand GG. 1994. Ultrastructural analysis of the invasion of tick cells by Lyme disease spirochetes (*Borrelia burgdorferi*) *in vitro*. Can J Zool 72:977–994. <https://doi.org/10.1139/z94-134>.